

# Local and anisotropic excitation of surface plasmon polaritons by semiconductor nanowires

T.M. Rümke<sup>1</sup>, J.A. Sánchez-Gil<sup>2</sup>, O.L. Muskens<sup>1</sup>, M.T. Borgström<sup>3</sup>,  
E.P.A.M. Bakkers<sup>3</sup>, and J. Gómez Rivas<sup>1,\*</sup>

<sup>1</sup>*FOM Institute for Atomic and Molecular Physics AMOLF, c/o Philips Research Laboratories, High Tech Campus 4, 5656 AE, Eindhoven, The Netherlands.*

<sup>2</sup>*Instituto de Estructura de la Materia, Consejo Superior de Investigaciones Científicas, Serrano 121, 28006 Madrid, Spain.*

<sup>3</sup>*Philips Research Laboratories, High Tech Campus 4, 5656 AE Eindhoven, The Netherlands*  
[j.gomez@amolf.nl](mailto:j.gomez@amolf.nl)

**Abstract:** We demonstrate a novel functionality of semiconductor nanowires as local sources for surface plasmon polaritons (SPPs). Photoexcited semiconductor nanowires decay non-radiatively exciting SPPs when they are on top of a metallic surface. We have investigated the anisotropic excitation of SPPs by nanowires by placing individual InP nanowires inside gold bullseye gratings. The gratings serve to couple SPPs to free space radiation that is detected with a scanning confocal microscope. The circular geometry of the grating allows to conclude that SPPs are preferentially generated in the direction along the nanowire axis.

© 2008 Optical Society of America

**OCIS codes:** (240.6680) Surface plasmons, (050.1950) Diffraction gratings, (260.3800) Luminescence.

---

## References and links

1. K. Haraguchi, T. Katsuyama, K. Hiruma, and K. Ogawa, "GaAs p-n junction formed in quantum wire crystals," *Appl. Phys. Lett.* **60**, 745-747 (1992).
2. M.H. Huang, S. Mao, H. Feick, H. Yan, Y. Wu, H. Kind, E. Weber, R. Russo, and P. Yang, "Room-temperature ultraviolet nanowire nanolasers," *Science* **292**, 1897-1899 (2001).
3. X. Duan, Y. Huang, R. Agarwal, and C.M. Lieber, "Single-nanowire electrically driven lasers," *Nature* **421**, 241-245 (2003).
4. E.D. Minot, F. Kelkensberg, M. van Kouwen, J.A. van Dam, L.P. Kouwenhoven, V. Zwiller, M.T. Borgström, O. Wunnicke, M.A. Verheijen, and E.P.A.M. Bakkers, "Single quantum dot nanowire LEDs," *Nano Lett.* **7**, 367-371 (2007).
5. M.T. Borgström, V. Zwiller, E. Müller, and A. Imamoglu, "Optically bright quantum dots in single nanowires," *Nano Lett.* **5**, 1439-1443 (2005).
6. J. Wang, M.S. Gudixsen, X. Duan, Y. Cui, and C.M. Lieber, "Highly polarized photoluminescence and photodetection from single indium phosphide nanowires," *Science* **293**, 1455-1457 (2001).
7. O.L. Muskens, M.T. Borgström, E.P.A.M. Bakkers, and J. Gómez Rivas, "Giant optical birefringence in ensembles of semiconductor nanowires," *Appl. Phys. Lett.* **89**, 233117 (2006).
8. B. Tian, X. Zheng, T.J. Kempa, Y. Fang, N. Yu, G. Yu, J. Huang, and C.M. Lieber, "Coaxial silicon nanowires as solar cells and nanoelectronic power sources," *Nature* **449**, 885-889 (2007).
9. W.L. Barnes, A. Dereux, and T.W. Ebbesen, "Surface plasmon subwavelength optics," *Nature* **421**, 824-830 (2003).
10. L. Yin, V.K. Vlaso-Vlasov, J. Pearson, J.M. Hiller, J. Hua, U. Welp, D.E. Brown, and C.W. Kimball, "Subwavelength focusing and guiding of surface plasmons," *Nano Lett.* **5**, 1399-1402 (2005).
11. H.L. Offerhaus, B. van de Bergen, M. Escalante, F.B. Segerink, J.P. Korterik, and N.F. van Hulst, "Creating focused plasmons by noncollinear phasematching on functional gratings," *Nano Lett.* **5**, 2144-2148 (2005).

12. F. Lopez-Tejeira, S.G. Rodrigo, L. Martin-Moreno, F.J. Garcia-Vidal, E. Devaux, T.W. Ebbesen, J.R. Krenn, I.P. Radko, S.I. Bozhevolnyi, M.U. Gonzalez, J.C. Weeber, and A. Dereux, "Efficient unidirectional nanoslit couplers for surface plasmons," *Nature Phys.* **3**, 324-328 (2007).
13. H. Raether, "Surface plasmons on smooth and rough surfaces and on gratings," (Springer, Berlin 1988).
14. W.L. Barnes, "Fluorescence near interfaces: the role of photonic mode density," *J. Mod. Opt.* **45**, 661-699 (1998).
15. G.W. Ford and W.H. Weber, "Electromagnetic interaction of molecules with metal surfaces," *Phys. Rep.* **113**, 195-287 (1984).
16. W. Knoll, M.R. Philpott, J.D. Swalen, and A. Girlando, "Emission of light from Ag metal gratings coated with dye monolayer assemblies," *J. Chem. Phys.* **75**, 4795-4799 (1981).
17. R.W. Gruhlke, W.R. Holland, and D.G. Hall, "Surface-plasmon coupling in molecular fluorescence near a corrugated thin metal film," *Phys. Rev. Lett.* **56**, 2838-2841 (1986).
18. O.L. Muskens, J. Treffers, M. Forcales, M.T. Borgström, E.P.A.M. Bakkers, and J. Gómez Rivas, "Modification of InP nanowire photoluminescence by coupling to surface plasmons on a metal grating," *Opt. Lett.* **32**, 2097-2099 (2007).
19. H.E. Ruda and S. Shik, "Polarization-sensitive optical phenomena in semiconducting and metallic nanowires," *Phys. Rev. B*, **72**, 115308:1-11 (2005).
20. J. A. Sánchez-Gil, "Coupling, resonance transmission, and tunneling of surface plasmon polaritons through metallic gratings of finite length," *Phys. Rev. B* **53**, 10317-10327 (1996).
21. J. A. Sánchez-Gil and M. Nieto-Vesperinas, "Light scattering from random rough dielectric surfaces," *J. Opt. Soc. Am. A* **8**, 1270-1286 (1991).
22. M. Kuttge, H. Kurz, J. Gómez Rivas, J.A. Sánchez-Gil, and P. Haring Bolivar, "Analysis of the propagation of terahertz surface plasmon polaritons on semiconductor groove gratings," *J. Appl. Phys.* **101**, 023707:1-6 (2007).

## 1. Introduction

The precise control on the growth and doping of semiconductor nanowires is leading to a tremendous increase of interest in these nanostructures as building blocks for nanoscale optical and optoelectronic devices. Semiconductor nanowires have proven their functionality as nano-LEDs and lasers [1, 2, 3, 4], single photon emitters [5], polarization sensitive detectors [6], polarization optics [7] and in photovoltaics [8].

Here we demonstrate a new functionality of semiconductor nanowires as local sources of surface plasmon polaritons (SPPs). SPPs are electromagnetic waves coupled to free charge carriers at the interface between a dielectric and a metal. The evanescent character of SPPs in the direction perpendicular to the interface can lead to subwavelength electromagnetic field confinement. This characteristic makes surface plasmon optics or plasmonics of great interest for nanoscale optics [9]. Plasmonic research has focused so far on the control of the propagation of SPPs, dedicating much less effort to the efficient generation of SPPs. However, a precise control of the spatial and angular emission of SPPs by plasmonic nanosources is necessary for the development of complex plasmonic circuits [10, 11, 12].

Due to momentum mismatch at every frequency, it is not possible to couple free-space electromagnetic radiation to SPPs. Two schemes broadly used to facilitate this coupling are grating assisted coupling and near-field coupling. With the first method, the momentum difference between SPPs and light is provided by scattering in the periodic structure defined by a grating [13]. Light scattered by the grating can gain or lose momentum with a magnitude equal to an integer number of the reciprocal lattice vector. This method provides large coupling efficiencies at certain frequencies determined by the angle of incidence of light onto the grating. A broadband method of excitation of SPPs is near-field coupling of light emitters close to metals [14]. If an emitter is located in the proximity of a metallic surface it can decay non-radiatively by exciting SPPs. This decay channel causes the quenching of the photoluminescence of light emitters at small distances to metal-dielectric interfaces [15]. By patterning the metal surface with a grating structure it is possible to couple the SPPs back to radiation emitted in certain directions [16, 17].

As we will show, efficient and local excitation of SPPs is possible using photoexcited semiconductor nanowires. Nanowires are structures with a diameter in the range of 10 to 100 nm

and with a length of several micrometers. The geometrical anisotropy of nanowires and the high refractive index of semiconductors translate into a large optical anisotropy: the dipole moment of nanowires is mainly oriented along their long axis, which leads to strongly polarized photoluminescence of individual nanowires with the polarization vector oriented along their axis [6]. Therefore, one might expect that the polarized emission of nanowires leads to an anisotropic excitation of SPPs when a nanowire is close to a metallic surface [18]. We have measured the anisotropic emission of SPPs as follows. Nanowires are placed inside gold bullseye gratings, which play the role of outcoupler for the excited SPPs. The detected light, coupled out by the grating at different positions, maps the SPP intensity on the surface at different angles with respect to the long axis of the nanowire. We find that nanowires generate SPPs preferentially in the direction along their long axis.

## 2. Sample Preparation

The bullseye gratings were fabricated by evaporating a gold layer with a thickness of 320 nm onto a silicon substrate. This thickness is much larger than the skin depth of gold  $\delta$  in the near infrared ( $\delta \simeq 10$  nm). It is therefore reasonable to consider the film as a semi-infinite gold layer. After evaporation of the gold we defined an array of  $18 \times 16$  bullseye gratings by milling grooves with a focus ion beam (FEI FIB200). The gratings have a lattice constant of 620 nm and are formed by 10 concentric grooves with a width of 300 nm and a depth of 100 nm. The radius of the innermost groove is  $5 \mu\text{m}$ . A photograph of the array of gratings taken with an optical microscope in a dark-field imaging mode is displayed in Fig. 1. The flat gold surface corresponds to the dark areas in the photograph. The array of bullseye gratings appears bright due to light scattered by the grooves into the dark field objective. The bright spots in Fig. 1 correspond to light scattered by the nanowires. The synthesis and deposition of the nanowires onto the sample is described next.

Indium phosphide nanowires were synthesized using the vapor-liquid-solid growth method in a metal-organic vapor phase epitaxy (MOVPE) reactor. A suspension of colloidal gold particles in water was spun onto a n-doped InP (111)B wafer. These particles served as catalyst for the growth. The wafer with colloids was placed in a laminar flow MOVPE reactor cell heated up to a temperature of  $420^\circ\text{C}$  at a pressure of 50 mbar. During this heating process, the sample

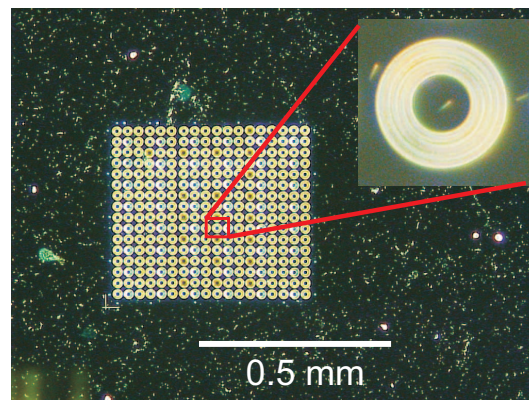


Fig. 1. Dark field optical microscope image of an array of  $18 \times 16$  bullseye gratings. The bright, dusty like, spots on the image correspond to the light scattered by InP nanowires. The inset displays a larger magnification image centered on a bullseye grating that contains an individual InP nanowire.

was kept under a constant phosphine ( $\text{PH}_3$ ) molar fraction of  $8.3 \times 10^{-3}$  using hydrogen as a carrier gas. The growth of the nanowires was initiated by introducing trimethylindium (TMI) with a molar fraction of  $0.3 \times 10^{-4}$  into the reactor cell. The diameter of the Au colloids defines to first approximation the diameter of the nanowires. The length is determined by the growth time. The average nanowire diameter and length are 50 nm and 2.3  $\mu\text{m}$  respectively.

After synthesis some nanowires were removed from the substrate by placing the sample in isopropanol and freezing it by immersion in liquid nitrogen. The different thermal expansion coefficients of bulk InP and InP nanowires led to the fracture of nanowires at their base, which gave rise, after melting the isopropanol, to a suspension of nanowires. A few drops of this suspension was put onto the grating array and the isopropanol was let to evaporate. The final sample consists of InP nanowires randomly dispersed onto the metal film structured with the gratings. After inspection of the array we found three bullseye gratings containing an individual nanowire. A higher-magnification dark-field microscope image of one of these gratings is displayed in the inset of Fig. 1. The data presented in this article corresponds to this specific nanowire. We found similar results for the other two gratings of the array, each containing an individual nanowire.

### 3. Optical Measurements

Firstly, we characterized the spectrum and polarization anisotropy of the emission of the nanowire with a micro-photoluminescence setup coupled to a high efficiency spectrometer (Andor-SR 303i). The photoluminescence is excited with light from an argon laser at a wavelength  $\lambda = 488$  nm, focused onto individual nanowires by means of a microscope objective (x50, NA=0.75). The photoluminescence was collected by the same objective and sent through a dichroic mirror to filter out the pump light and through a polarization filter before detection. The polarizer was aligned with its transmission axis parallel or perpendicular to the long axis of the nanowire. Figure 2 displays the photoluminescence spectra of a single nanowire. The solid curve in this figure corresponds to the intensity measured with the polarizer parallel to the long axis of the nanowire, while the dashed curve is the intensity polarized perpendicular to this axis. In agreement with previous experimental and theoretical results [6, 19], the emission of individual nanowires is strongly polarized in the direction along their long axis. This anisotropy is caused by the small lateral dimensions of the nanowires and the large dielectric contrast between the nanowires and their surroundings [19]. Due to the collection optics of the micro-photoluminescence setup, there is a polarization component perpendicular to the long axis of the nanowire (along its vertical dimension) detected when the polarization filter is set parallel to this axis and the photoluminescence is emitted in the plane defined by the nanowire axis and the normal to the surface of the substrate. However, the relatively low numerical aperture of the objective used in these measurements makes this contribution residual as it is apparent by the large polarization anisotropy in the emission of Figure 2.

We used a scanning confocal microscope to investigate the excitation of SPPs by individual nanowires. A schematic representation of the setup is presented in Fig. 3. The photoluminescence of the nanowire was excited by illumination with light from a laser diode at a wavelength of 660 nm. Note that this excitation wavelength differs from that used to measure the spectra of Fig. 2 due to the available laser sources in these two independent setups. Although one may expect a slightly different polarization anisotropy on the emission at different wavelengths due to the dispersion of InP [19], this difference will be minor as compared to reported wire to wire variations of the polarization anisotropy due to small changes in the nanowire diameter [18]. The  $\lambda = 660$  nm excitation light, incident under an angle of  $60^\circ \pm 5^\circ$  with respect to the surface normal, was focused to an elliptical spot with a long axis of  $\simeq 12 \mu\text{m}$  and a short axis of  $\simeq 6 \mu\text{m}$  using a set of focusing lenses. In this way the excitation spot was fixed, i.e., it was not

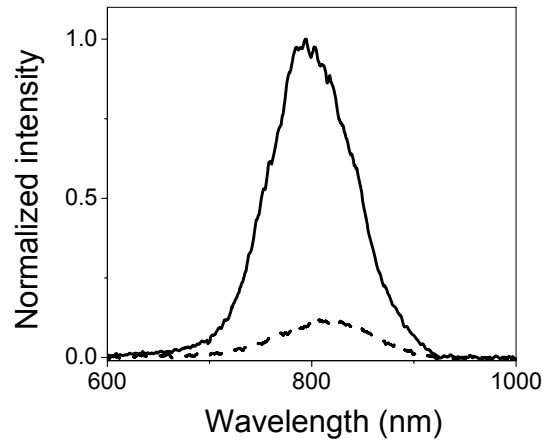


Fig. 2. Photoluminescence spectrum of light emitted by an InP nanowire measured with a polarization parallel (solid line) and perpendicular (dashed line) to its long axis.

sent through the scanning confocal system. The direct photoluminescence from the nanowire and the SPPs excited by the nanowire and coupled out by the grating were collected by a 50x objective with a working distance of 3 mm and a numerical aperture of 0.7. The laser light was filtered out by a dichroic filter with a cut-off wavelength of 700 nm. A polarizer in the detection path allowed the selection of the polarization state. A set of computer-controlled scanning mirrors on the optical detection path scanned the point of observation onto the surface with a resolution limited by diffraction. Therefore, it was possible to obtain spatially resolved information of the emitted SPPs by the nanowire coupled out at different positions by the circular grating. Note that even though the excitation spot onto the surface had a size in the order of the size of the bullseye grating, the photoluminescence and SPPs detected were generated by the nanowire as this was the only optically active element in the illuminated area.

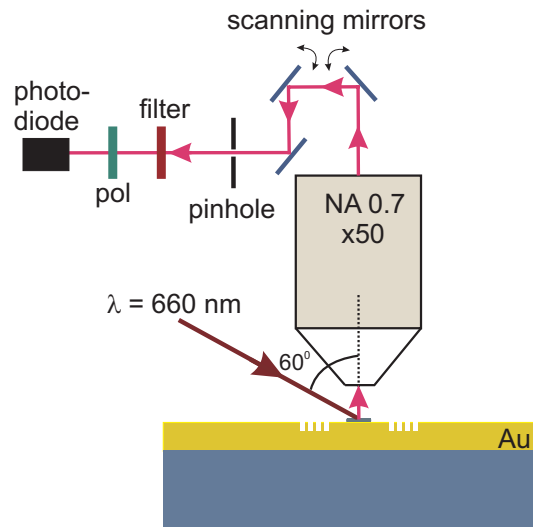


Fig. 3. Experimental setup used to investigate the excitation of SPPs by a semiconductor nanowire.

Figure 4 displays the spatially resolved intensity emitted by the nanowire inside the circular grating. Figure 4(a) is a microscope image of the nanowire inside the bullseye grating. Figure 4(b) corresponds to the intensity measured with a polarization parallel to the long axis of the nanowire, while Fig. 4(c) displays the intensity polarized perpendicular to the nanowire axis. The directions of the polarization vector are indicated by the dashed lines in Figs. 4(b) and (c). The central bright spot in these figures corresponds to the photoluminescence directly emitted from the nanowire. In agreement with Fig. 2, this photoluminescence is mainly polarized along the long axis of the nanowire. Bright bands are observed in Figs. 4(b) and (c) clearly separated from the central nanowire and corresponding to the position of the circular grating. These bands are attributed to SPPs generated by the non-radiative decay of the excited nanowire on the proximity of the metal surface. The SPPs propagate along the flat metal-air interface reaching the circular grating, which couples them out into free-space radiation that is collected by the objective and detected. This radiation is emitted at an angle  $\theta$  with respect to the surface normal given by the momentum matching condition [13]

$$k_0 \sin \theta \pm nG = \pm k_{SPP}, \quad (1)$$

where  $k_0$  is the wave vector of free space radiation,  $k_{SPP} \simeq k_0 \sqrt{\epsilon_m / (\epsilon_m + 1)}$  is the wave vector of the SPPs on the grating, being  $\epsilon_m$  the permittivity of gold,  $G = 2\pi/d$  is the reciprocal lattice vector, with  $d$  the period of the grating, and  $n$  an integer indicating the diffractive order. Therefore, for a grating with a period of 620 nm and at the wavelengths of emission of InP nanowires, i.e., between 700 and 900 nm, SPPs are only coupled into the first diffractive order at angles smaller than  $26^\circ$  with respect to the normal of the sample. This maximum angle of outcoupling is smaller than the acceptance angle of the objective. Consequently, all SPPs coupled out by the grating to far-field radiation are collected and detected.

As can be appreciated in Fig. 4, SPPs are preferentially excited in the direction defined by the long axis of the nanowire. To better quantify this anisotropic excitation of SPPs we display in Fig. 5 a polar plot of the normalized SPP intensity measured with unpolarized detection on a circle with radius equal to the innermost radius of the circular grating. This circle is marked with the thin dotted curve in Fig. 4(b). The orientation of the nanowire in this polar plot is along the horizontal direction on which the maximum SPP emission takes place. These measurements

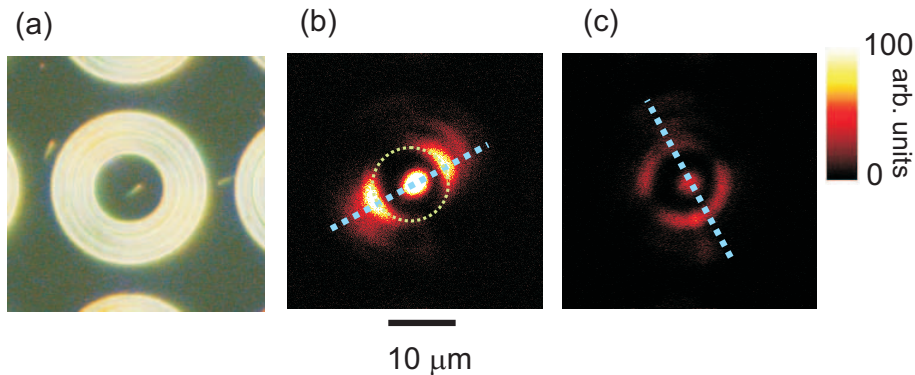


Fig. 4. (a) Optical microscope image of an InP nanowire inside a bullseye grating. Photoluminescence images measured with a polarization parallel to the long axis of the nanowire (b) and perpendicular to this axis (c). The polarization state is indicated by the dashed lines. The thin dotted circle in (b) indicates the innermost groove of the circular grating and the positions at which the polar plot of the SPP emission of Fig. 5 is obtained.

support the interpretation of the intensity measured in the grating as corresponding to SPPs excited by the nanowire and coupled out by the grating, and rules out an interpretation in terms of light emitted by the nanowire propagating grazing to the surface and scattered out by the grating. If the measurements were due to this radiation propagating grazing to the surface one should expect a maximum intensity at positions perpendicular to the polarization direction of the emission, i.e., perpendicular to the long nanowire axis. On the other hand SPPs are longitudinal surface waves, i.e., the projection of the polarization vector of SPPs on the surface is parallel to their propagating wave vector. Therefore, one may expect that the anisotropy of semiconductor nanowires with a polarized emission along their long axis determines a directional excitation of SPPs in the same direction, as it is indeed observed in the measurements. This argument can be also used to attribute the bright band of Fig. 4(c) to SPPs excited by the weaker nanowire emission perpendicular to the nanowire axis and coupled out by the grating, rather than to grazing radiating scattered by the grating. Grazing radiation directly emitted by the nanowire is mainly polarized along the long axis of the nanowire and will be emitted in the direction perpendicular to this axis. This polarization is however blocked by the polarization filter used to obtain the measurement of Fig. 4(c).

Figure 6(a) displays the normalized intensity along the dashed line of Fig. 4(b). A distance equal to zero corresponds to the center of the bullseye grating. Note that the nanowire is not exactly located at the center of the bullseye as can be appreciated by the small shift of the central maximum of Fig. 6(a). This central maximum is the direct photoluminescence emitted by the nanowire, while the two maxima of lower intensity at both sides are the SPP intensity coupled out to radiation by the grating. The ratio of the direct nanowire emission to the SPP emission, obtained from Fig. 6(a) by integrating the intensities of the different peaks, reaches the value of 1.3. These similar intensities highlight the efficient excitation of SPPs by nanowires located on top of metallic surfaces.

To analyze further the excitation of SPPs by nanowires, we have carried out theoretical calculations that confirm the nature of this excitation. For simplicity, we consider a system consisting of a sinusoidal grating instead of a nanowire used to excite SPPs. A Gaussian beam impinges on the grating at  $\theta_0 = 30^\circ$  and is coupled to a backward propagating SPP as imposed by the Bragg diffraction condition for the -1-order (period  $d$  fulfils  $k_{SPP} = (2\pi/d) - (\omega/c) \sin \theta_0$ ). The

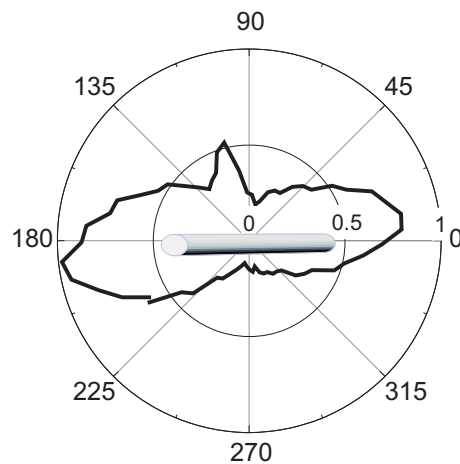


Fig. 5. Polar plot of the normalized SPP emission at the innermost groove of the circular grating. The nanowire, which is represented schematically inside the plot, is oriented with its long axis along the horizontal direction.

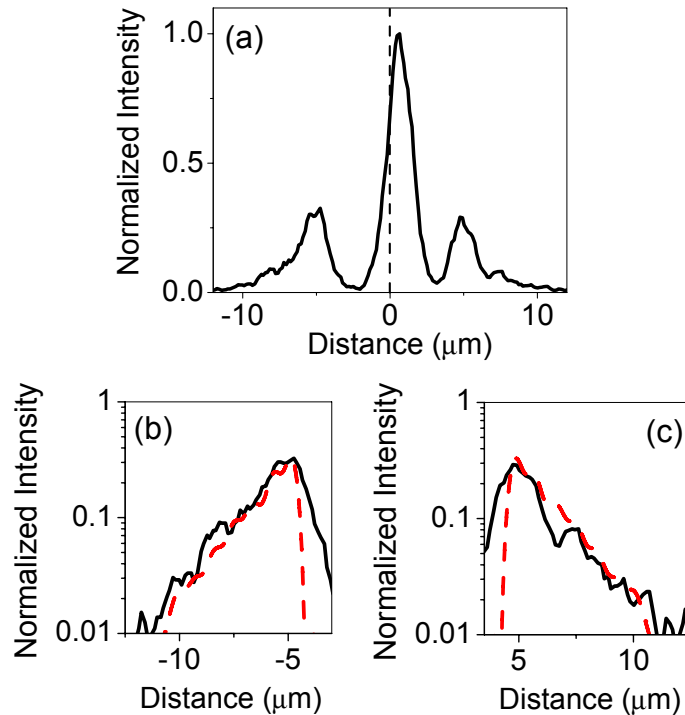


Fig. 6. (a) Normalized intensity of the photoluminescence of Fig. 4(a) along the dashed line in this figure. (b) and (c) are a close up to the two maxima at the sides of the direct photoluminescence of the nanowire (central maximum in (a)). The red-dashed curves in (b) and (c) correspond to the calculated SPP confocal intensity coupled out by a grating with the same geometrical parameters as the one used for the experiment.

resulting SPP propagates through a flat region and is subsequently scattered by a groove array. The length of the flat region and the groove array parameters are chosen in the 2D calculations similar to the radial dependence of the circular grating in the experiment. Calculations have been carried out by means of the exact Green's theorem surface integral equations, making use of the impedance boundary condition on a curved surface to further simplify the surface electromagnetic fields. The details of the calculation can be found in Ref. [20]. In order to simulate the measured confocal microscopy intensity, the surface electric field obtained with the above formulation has been filtered in the following manner: First, the angular spectrum representation is obtained [21]; then the evanescent components are filtered out, as well as those propagating components beyond the numerical aperture of the microscope objective, finally the resulting components are used to retrieve the surface electric field that is plotted in Figs. 6(b) and (c) with red-dashed curves. Thus the flat region, which corresponds to distances between  $-5$  and  $5 \mu\text{m}$  in Figs. 6(b) and (c), appears dark despite that the surface electric field intensity is not zero for the propagating SPPs: Due to the evanescent nature of SPPs, their contribution to the confocal signal is negligible. When the SPP hits the groove array, it is coupled out by the grating, and the resulting out-of-plane components are observed through the confocal microscope. The numerical calculations confirm this SPP coupling and predict an exponentially decaying out-of-plane scattering with a decay length  $l_{out} \approx 2\mu\text{m}$ , in agreement with the measured decay in the intensity (black lines in Figs. 6(b) and (c)). Note that this decay length is much shorter than the propagation length of SPPs on flat surfaces as it is mainly determined by the scattering

of SPPs in the grooves defining the grating. The SPP scattering strength depends on the size of the scatterers [22] and can be large in gratings with deep grooves as those used in our experiments, reducing significantly the SPP propagation length. No fitting parameters have been used in the calculations of Figs. 6(b) and (c), and the good agreement between calculation and experiments confirms our interpretation of the measurements in terms of the excitation of SPPs by the semiconductor nanowire, being coupled out to radiation by the grating.

#### **4. Conclusion**

By placing individual InP nanowires inside bullseye gratings structured on an Au-air interface, we have investigated the excitation of SPPs by semiconductor nanowires. The large polarization anisotropy in the photoluminescence of nanowires gives rise to an anisotropic excitation of SPPs. Surface plasmon polaritons are mainly excited in the direction of the long axis of the nanowire. Semiconductor nanowires may find new functionalities as nanosources in plasmonic circuits. The possibility of doping nanowires to form p-n junctions and the ease to contact these nanostructures may also lead to electrically driven sources of SPPs.

#### **Acknowledgments**

We acknowledge R.G.R. Weemaes and H.A.G. Nulens for technical assistance. J.A.S.-G. acknowledge partial support from the Spanish Ministerio de Educación y Ciencia (grant FIS2006-07894) and Comunidad de Madrid through the MICROSERES network (grant S-0505/TIC-0191). This work is part of the research program of the Stichting voor Fundamenteel Onderzoek der Materie (FOM), which is financially supported by the Nederlandse Organisatie voor Wetenschappelijk Onderzoek (NWO), and is part of an industrial partnership program between Philips and FOM.